NJIT CAMS Technical Report:

Mixed-mode oscillations in single neurons *

Horacio G. Rotstein
Department of Mathematical Sciences
New Jersey Institute of Technology
Newark, NJ 07102, USA

October 22, 2013

Definition

Mixed-mode oscillations (MMOs) in neuronal systems are oscillatory patterns of activity consisting of subthreshold (or membrane potential) oscillations interspersed with action potentials (or spikes).

Detailed Description

Introduction

Rhythmic oscillations in the theta (4-12 Hz) and gamma (30 - 100 Hz) frequency bands have been recorded in the hippocampus and the entorhinal cortex, and have been implicated in cognitive processes including memory, spatial navigation and sleep (Buzsáki 2002, 2006; Kahana et al. 1999; O'Keefe and Recce 1993; Traub and Whittington 2010; Buzsáki and Wang 2010; Engel et al. 2003; Fries 2009; Singer and Gray 1995; Bragin et al. 1995; Montgomery and Buzsaki 2007). These network oscillations emerge from the cooperative activity of the participating neurons and network connectivity.

Intrinsic subthreshold (membrane potential) oscillations (STOs) and MMOs at theta and gamma frequencies have been observed in various neuron types (Alonso and Llinás 1989; Dickson et al. 2000b,a; Leung and Yim 1991; Fransén et al. 2004; Schmitz et al. 1998; Yoshida and Alonso 2007; Bourdeau et al. 2007; García Munoz et al. 1993; Llinás et al. 1991). MMOs have been most notably investigated in stellate cells in layer II of the medial entorhinal cortex (Fransén et al. 1998; Fernandez and White 2008; Giocomo et al. 2007; Yoshida and Alonso 2007).

*To be published in the Encyclopedia of Computational Neuroscience

Several models have been used to investigate MMOs (Wang 2002; White et al. 1998; Fransén et al. 2004; Acker et al. 2003; Rotstein et al. 2006, 2008; Jalics et al. 2010; Medvedev and Cisternas 2004; Dorval and White 2005; Brøns et al. 2008; Desroches et al. 2012; Morin et al. 2010). These models focus on the role of the ionic currents in shaping the MMO patterns (generation of STOs and the onset of spikes) or the dynamic mechanisms that give rise to MMOs.

The functionality of MMOs is still a matter of discussion. STOs have been argued to function as a timing device (Lampl and Yarom 1993) and to play a role in spatial navigation (Giocomo et al. 2007). While action potentials (or spikes) are the basic neuronal signaling mechanism (Johnston and Wu 1995; Koch 1999; Dayan and Abbott 2001; Ermentrout and Terman 2010), the interspersed STOs in the MMO patterns (Figs. 1 and 2) may help create a time scale at which information is effectively communicated among neurons.

The structure of MMO patterns

Typically, a MMO cycle consists of s small amplitude oscillations followed by L spikes (or vice versa). The notation L^s is customarily used to described these patterns (Desroches et al. 2012; Brøns et al. 2008) (and papers therein). MMO patterns can be regular (Figs. 1-A and -B) or irregular (Fig. 1-C). In turn, regular MMO patterns can be uniform, where the sequence L^s describes the MMO patterns in their entirety (Fig. 1-A), or non-uniform, where MMO cycles consists of sub-cycles described by sequences $L_1^{s_1} - L_2^{s_2} - \ldots - L_N^{s_N}$ (for some integer N) (Fig. 1-B). Irregular MMO patterns can be either stochastic (Fig. 1-C) or chaotic (not shown).

The occurrence of L^0 cycles (for $L > 1$) embedded in MMO patterns, with two or more consecutive spikes with no interspersed STOs (Figs. 1-B2, B5 and -C), is customarily referred to as spike clustering (Fransén et al. 2004; Alonso and Klink 1993; White et al. 1998; Serafin et al. 1996; Desmaisons et al. 1999; Wang 2002; Muratov and Vanden-Eijnden 2008; Kuske and Borowski 2009). The inter- and intra-spike frequency may belong in the same frequency range or not depending on the neuronal type and other parameter values.

Dynamic mechanisms of generation of MMOs

The generation of MMO patterns requires the coordinated action of various mechanisms: (i) a mechanism for the generation of STOs, (ii) a spiking mechanism, including the onset of spikes and the description of the spiking dynamics, and (iii) a return mechanism from the spiking regime back to the subthreshold regime.

The minimal models able to generate intrinsic oscillatory behavior are 2D and involve the dynamics of the voltage v and a recovery variable (w) (Rinzel and Ermentrout 1998; Rinzel 1985; Ermentrout and Terman 2010; Rinzel and Ermentrout 1998; Ermentrout and Kopell 1998; FitzHugh 1961; Nagumo et al. 1962). These models may generate either STOs (Fig. 3-A) or spikes (Fig. 3-B) but not MMOs. MMO patterns require an additional mechanism that describes the dynamic transition between these two regimes. This mechanism may be provided by an external input (non-autonomous system), such as in certain cases of the slow passage through a Hopf bifurcation (Holden and Erneux 1993; Baer et al. 1989) and the patterns resulting from oscillatory forcing (Barnes and Grimshaw 1997; Shimizu et al. 2012), or by an additional dependent variable (autonomous system) (Fig. 3-C) as in the 3D canard phenomenon (Wechselberger 2005; Brøns et al. 2006).

The minimal models that are able to generate intrinsic MMOs are nonlinear, 3D and involve multiple time scales. The prototypical example is the 3D extended version of the FitzHugh-Nagumo (FHN) model (FitzHugh 1961; Nagumo et al. 1962) (Fig. 3) describing the dynamics of the voltage v and two gating variables (w and z) with linear dynamics. Models of FHN type are caricature models, but they capture the basic dynamic properties observed in detailed biophysical (conductance-based) models.

In the example presented in Fig. 3 all the MMO mechanisms are described by the same model. The generation of STOs (Fig. 3-A3) and the onset of spikes (Fig. 3-B3) are governed by the locally parabolic portion of the v-nullcline, near its minimum. The spiking dynamics and the return mechanisms are primarily governed by the right and left branches of the v-nullcline respectively (Fig. 3-A2). The abrupt transition from STOs to spikes is due to the 2D (Figs. 3-A and -B) and 3D canard phenomena (Figs. 3-C) (Krupa and Szmolyan 2001; Wechselberger 2005; Brøns et al. 2006). The locally parabolic nonlinearity at the minimum of the v-nullcline and the time scale separation between v and the remaining dependent variables are key for these mechanisms.

Higher dimensional models provide the necessary flexibility for the generation of more complex MMO patterns. Typically, in these models each mechanism (e.g., STOs, spikes) is described by a different, lower-dimensional regime (Rotstein et al. 2006).

Generalizations of the integrate-and-fire model to include 2D linear subthreshold dynamics (Izhikevich 2001; Richardson et al. 2003; Rotstein 2013) are able to produce MMOs provided the fixed-point of the underlying (subthreshold) 2D linear system is an unstable focus (Rotstein 2013). (Stable foci are possible in the stochastic case.) These models are referred to as STO-F models (STO-and-fire models) (Rotstein 2013). The mechanism of spike generation consists of a voltage threshold (V_{th}) and "artificial spikes": spikes are added manually when the voltage V crosses V_{th}. The return mechanism consists on the manual reset of V and w to predetermined values V_{rst} and w_{rst} after a spike has occurred. STO-F models with constant values of w_{rst} generate regular uniform 1^s MMO patterns (Fig. 1-A) where the number of STOs per cycle depends on the model parameters. The generation of regular non-uniform MMO patterns requires a return mechanism where at least one reset value (either V_{rst} or w_{rst}) is not constant, and depends, for instance, on the number of consecutive spikes within some range (Fig. 1-B).

Generalizations of the integrate-and-fire model to include 2D or 3D nonlinear subthreshold dynamics, such as the reduced medial entorhinal cortex layer II stellate cell model (Rotstein et al. 2006) and extensions of the quadratic-integrate-and-fire models (Izhikevich 2001, 2006; Rotstein et al. 2006, 2008; Jalics et al. 2010), typically have a parabolic-like V-nullcline in the subthreshold regime and the gating variables have either linear or sigmoidal nullclines (Izhikevich 2001, 2010; Rotstein et al. 2006). These models are able to generate STOs provided the fixed-point in the subthreshold regime is a focus. In addition, these models describe the onset of spikes, but not the spiking dynamics. The voltage threshold V_{th} indicates the occurrence of spikes, which are added manually. (Note that V_{th} is not a part of the spiking generation mechanism.) The voltage and possibly the gating variables are reset after a spike has occurred (return mechanism). In principle, MMOs are possible when the subthreshold dynamics are 2D provided the reset point (V_{rst}, w_{rst}) is close enough to the fixed-point and the latter is unstable, thus generating a spiraling out solution. However, for biophysically plausible situations, this condition is not satisfied, and an additional subthreshold variable (z) is required to govern the dynamic transition from STOs to spikes (Fig. 2). The slow component of the h-current plays this role in the stellate cell model mentioned above

(Rotstein et al. 2006, 2008), while a persistent sodium and the fast component of the h-current are enough to generate STOs.

The mechanisms of generation of MMOs in conductance-based models when different sets of ionic currents govern the dynamics of the subthreshold and spiking regimes are more difficult to analize due to their high dimensionality. There are circumstances where the dynamics for different regimes can be treated separately by using reduction of dimensions methods (Rotstein et al. 2006).

The mechanism of generation of MMOs crucially depends on the mechanism of transition from STOs to spikes. Several mechanisms have been described in the literature (Guckenheimer et al. 1997; Wechselberger 2005; Guckenheimer 2008a,b; Krupa and Wechselberger 2010; Koper 1995; Larter and Steinmetz 1991) in addition to the canard phenomenon (Szmolyan and Wechselberger 2001; Wechselberger 2005; Brøns et al. 2006; Rotstein et al. 2006) and the slow passage through a Hopf bifurcation (Larter et al. 1988; Holden and Erneux 1993; Baer et al. 1989) . These mechanisms are reviewed in (Desroches et al. 2012).

We note that MMOs have also been observed in other fields including chemistry and biology (Petrov et al. 1992; Aguda et al. 1989; Hauser and Olsen 1996; Strizhak et al. 2002; Baba and Krischer 2008). In these cases MMOs consists of an alternation of small amplitude oscillations (SAOs) and large amplitude oscillations (LAOs) where the amplitude between SAOs and LAOs differ roughly by an order of magnitude.

Further Reading

Focus Issue on Mixed-Mode Oscillations, Chaos (2008) Brøns et al. (2008).

SIAM Review Desroches et al. (2012).

Acknowledgments

The author wishes to thank Martin Wechselberger and Frances Skinner for comments on this manuscript. This work was supported by NSF grants DMS-1313861 (HGR) and DMS-0817241 (HGR).

References

Acker CD, Kopell N, and White JA, Synchronization of strongly coupled excitatory neurons: Relating network behavior to biophysics. *Journal of Computational Neuroscience* 15: 71–90, 2003.

Aguda BD, Larter R, and Clarke B, Dynamic elements of mixed-mode oscillations and chaos in a peroxidase-oxidase model network. *J Chem Phys* 90: 4168–4175, 1989.

Alonso AA and Klink R, Differential electroresponsiveness of stellate and pyramidal-like cells of medial entorhinal cortex layer II. *J Neurophysiol* 70: 144–157, 1993.

Alonso AA and Llinás RR, Subthreshold Na^+-dependent theta like rhythmicity in stellate cells of entorhinal cortex layer II. *Nature* 342: 175–177, 1989.

Baba N and Krischer K, Mixed-mode oscillations and cluster patterns in an electrochemical relaxation oscillator under galvanostatic control. *Chaos* 18: 015103, 2008.

Baer SM, Erneux T, and Rinzel J, The slow passage through a Hopf bifurcation: Delay, memory effects, and resonance. *SIAM J Appl Math* 49: 55–71, 1989.

Barnes B and Grimshaw R, Numerical studies of the periodically forced bonhoeffer van der pol system. *Int J Bif Chaos* 7: 2653–2689, 1997.

Bourdeau M, Morin F, Laurent C, Azzi M, and Lacaille J, Kv4.3-mediated A-type K^+ currentes underlie rhythmic activity in hippocampal interneurons. *J Neurosci* 27: 1942–1953, 2007.

Bragin A, Jando G, Nadasdy Z, Hetke J, Wise K, and Buzsáki G, Gamma (40-100 hz) oscillation in the hippocampus of the behaving rat. *J Neurosci* 15: 47–60, 1995.

Brøns M, Kaper TJ, and Rotstein HG, Introduction to focus issue: Mixed mode oscillations: Experiment, computation, and analysis. *Chaos* 18: 015101, 2008.

Brøns M, Krupa M, and Wechselberger M, Mixed mode oscillations due to the generalized canard phenomenon. *in Fields Institute Communications* 49: 39–63, 2006.

Buzsáki G, Theta oscillations in the hippocampus. *NEURON* 33: 325–340, 2002.

Buzsáki G, *Rhythms of the brain*. Oxford University Press, 2006.

Buzsáki G and Wang XJ, Mechanisms of gamma oscillations. *Annu Rev Neurosci* 35: 203–225, 2010.

Dayan P and Abbott LF, *Theoretical Neuroscience*. The MIT Press, Cambridge, Massachusetts, 2001.

Desmaisons D, Vincent JD, and Lledo PM, Control of action potential timing by intrinsic subthreshold oscillations in olfactory bulb output neurons. *J Neurosci* 19: 10727–10737, 1999.

Desroches M, Guckenheimer J, Krauskopf B, Kuehn C, Osinga HM, and Wechselberger M, Mixed-mode oscillations with multiple time scales. *SIAM Reviews* 54: 211–288, 2012.

Dickson CT, Magistretti J, Shalinsky M, Hamam B, and Alonso AA, Oscillatory activity in entorhinal neurons and circuits. *Ann NY Acad Sci* 911: 127–150, 2000a.

Dickson CT, Magistretti J, Shalinsky MH, Fransén E, Hasselmo M, and Alonso AA, Properties and role of I_h in the pacing of subthreshold oscillation in entorhinal cortex layer II neurons. *J Neurophysiol* 83: 2562–2579, 2000b.

Dorval ADJ and White JA, Channel noise is essential for perithreshold oscillations in entorhinal stellate neurons. *J Neurosci* 25: 10025–10028, 2005.

Engel AK, Fries P, and Singer W, Dynamic predictions and synchrony in top-down processing. *Nat Rev Neurosci* 421: 844–848, 2003.

Ermentrout BG and Kopell N, Fine structure of neural spiking and synchronization in the presence of conduction delays. *Proc Natl Acad Sci USA* 95: 1259–1264, 1998.

Ermentrout GB and Terman D, *Mathematical Foundations of Neuroscience*. Springer, 2010.

Fernandez R and White JA, Artificial synaptic conductances reduce subthreshold oscillations and periodic firing in stellate cells of the entorhinal cortex. *J Neurosci* 28: 3790–3803, 2008.

FitzHugh R, Impulses and physiological states in models of nerve membrane. *Biophysical J* 1: 445–466, 1961.

Fransén E, Alonso AA, Dickson CT, and Magistretti ME J Hasselmo, Ionic mechanisms in the generation of subthreshold oscillations and action potential clustering in entorhinal layer II stellate neurons. *Hippocampus* 14: 368–384, 2004.

Fransén E, Dickson CT, Magistretti J, Alonso AA, and Hasselmo ME, Modeling the generation of subthreshold membrane potential oscillations of entorhinal cortex layer II stellate cells. *Soc Neurosci Abstr* 24: 814.815, 1998.

Fries P, Neuronal gamma-band synchronization as a fundamental process in cortical computation. *Annu Rev Neurosci* 32: 209–224, 2009.

García Munoz A, Barrio LC, and Buno W, Membrane potential oscillations in CA1 hippocampal pyramidal neurons *in vitro*: Intrinsic rhythms and fluctuations entrained by sinusoidal injected current. *Exp Brain Res* 97: 325–333, 1993.

Giocomo LM, Zilli EA, Fransén E, and Hasselmo ME, Temporal frequency of subthreshold oscillations scales with entorhinal grid cell field spacing. *Science* 315: 1719–1722, 2007.

Guckenheimer J, Return maps of folded nodes and folded saddle-nodes. *Chaos* 18: 015108, 2008a.

Guckenheimer J, Singular hopf bifurcation in systems with two slow variables. *SIAM J Appl Dyn Syst* 7: 1355–1377, 2008b.

Guckenheimer J, Harris-Warrick R, J P, and Willms A, Bifurcation, bursting and spike frequency adaptation. *Journal of Computational Neuroscience* 4: 257–277, 1997.

Hauser MJB and Olsen LF, Mixed-mode oscillations and homoclinic chaos in an enzyme reaction. *J Chem Soc Faraday Trans* 92: 2857–2863, 1996.

Holden L and Erneux T, Slow passage through a Hopf bifurcation: From oscillatory to steady state solutions. *SIAM J Appl Math* 53: 1045–1058, 1993.

Izhikevich E, *Dynamical Systems in Neuroscience: The geometry of excitability and bursting*. MIT Press (Cambridge, Massachusetts), 2006.

Izhikevich EM, Resonate-and-fire neurons. *Neural Networks* 14: 883–894, 2001.

Izhikevich EM, Hybrid spiking models. *Philos Trans R Soc A* 368: 5061–5070, 2010.

Jalics J, Krupa M, and Rotstein HG, A novel mechanism for mixed-mode oscillations in a neuronal model. *Dynamical Systems: An International Journal* 25: 445–482, 2010.

Johnston D and Wu SMS, *Foundations of cellular neurophysiology*. The MIT Press, Cambridge, Massachusetts, 1995.

Kahana MJ, Sekuler R, Caplan JB, Kirschen M, and Madsen JR, Human theta oscillations exhibit task dependence during virtual maze navigation. *Nature* 399: 781–784, 1999.

Koch C, *Biophysics of Computation*. Oxford University Press, 1999.

Koper MTM, Bifurcations of mixed-mode oscillations in a three variable autonomous van der Pol-Duffing model with a cross-shaped phase diagram. *Physica D* 80: 72–94, 1995.

Krupa M and Szmolyan P, Extending geometric singular perturbation theory to nonhyperbolic points - fold and canard points in two dimensions. *SIAM J Math Anal* 33(2): 286–314, 2001.

Krupa M and Wechselberger M, Local analysis near a folded saddle-node singularity. *J Differential Equations* 248: 2841–2888, 2010.

Kuske R and Borowski P, Survival of subthreshold oscillations: the interplay of noise, bifurcation structure, and return mechanism. *Discrete and Continuous Dynamical Systems* 4: 873–895, 2009.

Lampl I and Yarom Y, Subthreshold oscillations of the membrane potential: A functional synchronizing and timing device. *J Neurophysiol* 70: 2181–2186, 1993.

Larter R and Steinmetz CG, Chaos via mixed mode oscillations. *Philos Trans R Soc London A* 337: 291–298, 1991.

Larter R, Steinmetz CG, and Aguda B, Fast-slow variable analysis of the transition to mixed-mode oscillations and chaos in the peroxidase reaction. *J Phys Chem* 89: 6506–6514, 1988.

Leung LS and Yim CY, Intrinsic membrane potential oscillations in hippocampal neurons in vitro. *Brain Res* 553: 261–274, 1991.

Llinás RR, Grace AA, and Yarom Y, *In vitro* neurons in mammalian cortical layer 4 exhibit intrinsic oscillatory activity in the 10- to 50-hz frequency range. *Proc Natl Acad Sci USA* 88: 897–901, 1991.

Medvedev GS and Cisternas JE, Multimodal regimes in a compartmental model of the dopamine neuron. *Physica D* 194: 333–356, 2004.

Montgomery SM and Buzsaki G, Gamma oscillations dynamically couple hippocampal CA3 and CA1 regions during memory task performance. *Proc Natl Acad Sci USA* 104: 14495–14500, 2007.

Morin F, Haufler D, Skinner FK, and Lacaille JC, Characterization of voltage-gated K^+ currents contributing to subthreshold membrane potential oscillations in hippocampal CA1 interneurons. *J Neurophysiol* 103: 3472–3489, 2010.

Muratov CB and Vanden-Eijnden E, Noise-induced mixed-mode oscillations in a relaxation oscillator near the onset of a limit cycle. *Chaos* 18: 015111, 2008.

Nagumo JS, Arimoto S, and Yoshizawa S, An active pulse transmission line simulating nerve axon. *Proc IRE* 50: 2061–2070, 1962.

O'Keefe J and Recce ML, Phase relationship between hippocampal place units and the EEG theta rhythm. *Hippocampus* 3: 317–330, 1993.

Petrov V, Scott SK, and Showalter K, Mixed-mode oscillations in chemical systems. *J Chem Phys* 97: 6191–6198, 1992.

Richardson MJE, Brunel N, and Hakim V, From subthreshold to firing-rate resonance. *J Neurophysiol* 89: 2538–2554, 2003.

Rinzel J, Excitation dynamics: Insights from simplified membrane models. *Fed Proc* 44: 2944–2946, 1985.

Rinzel J and Ermentrout GB, Analysis of neural excitability and oscillations. *In Methods in Neural Modeling Koch, C and Segev, I, editors, second edition MIT Press: Cambridge, Massachusetts* 251–292, 1998.

Rotstein HG, Abrupt and gradual transitions between low and hyperexcited firing frequencies in neuronal models with fast synaptic excitation: A comparative study. *In Press* 2013.

Rotstein HG, Oppermann T, White JA, and Kopell N, A reduced model for medial entorhinal cortex stellate cells: Subthreshold oscillations, spiking and synchronization. *Journal of Computational Neuroscience* 21: 271–292, 2006.

Rotstein HG, Wechselberger M, and Kopell N, Canard induced mixed-mode oscillations in a medial entorhinal cortex layer II stellate cell model. *SIAM J Appl Dyn Sys* 7: 1582–1611, 2008.

Schmitz D, Gloveli T, Behr J, Dugladze T, and Heinemann U, Subthreshold membrane potential oscillations in neurons of deep layers of the entorhinal cortex. *NEURON* 85: 999–1004, 1998.

Serafin M, Williams S, Khateb A, Fort P, and Muhlethaler M, Rhythmic firing of medial septum non-cholinergic neurons. *Neuroscience* 75: 671–675, 1996.

Shimizu K, Saito Y, Sekikawa M, and Inaba N, Complex mixed-mode oscillations in a bonhoeffervan der pol oscillator under weak periodic perturbation. *Physica D* 18: 1518–1526, 2012.

Singer W and Gray C, Visual feature integration and the temporal correlation hypothesis. *Annu Rev Neurosci* 18: 555–586, 1995.

Strizhak PE, Khavrus VO, and Bar-Eli K, Effect of NO, CO, and Cl_2 on mixed-mode regimes in the Belousov-Zhabotinskyi oscillating chemical reaction in a cstr. *J Phys Chem* 106: 2505–2511, 2002.

Szmolyan P and Wechselberger M, Canards in $\mathbf{r}^3$. *J Diff Eq* 177: 419–453, 2001.

Traub RD and Whittington MA, *Cortical Oscillations in Health and Disease*. Oxford University Press, 2010.

Wang XJ, Pacemaker neurons for the theta rhythm and their synchronization in the septohippocampal reciprocal loop. *J Neurophysiol* 87: 889–900, 2002.

Wechselberger M, Existence and bifurcation of canards in R^3 in the case of a folded node. *SIAM J Appl Dyn Syst* 4: 101–139, 2005.

White JA, Klink R, Alonso A, and Kay AR, Noise from voltage-gated ion channels may influence neuronal dynamics in the entorhinal cortex. *J Neurophysiol* 80: 262–269, 1998.

Yoshida M and Alonso A, Cell-type-specific modulation of intrinsic firing properties and subthreshold membrane oscillations by the M(Kv7)-currents in neurons of the entorhinal cortex. *J Neurophysiol* 98: 2779–2994, 2007.

Figure Legends

Figure 1. MMO patterns in a 2D STO-F mode with linear subthreshold dynamics (see also resonate-and-fire models (Izhikevich 2001)). The subthreshold dynamics and governed by the following two equations describing the dynamics of the rescaled voltage V (mV) and gating variable w (mV) (see (Richardson et al. 2003)): (i) $CdV/dt = -g_L V - gw + I_{app}$, and (ii) $\tau\, dw/dt = v - w$. Spikes are added manually when V reaches V_{th} and V and w are reset to V_{rst} and w_{rst} respectively. **A.** The reset values V_{rst} and w_{rst} are constant and independent of the number of spikes. **A1.** $I_{app} = -0.2$. **A2.** $I_{app} = 0$. **A3.** $I_{app} = 0.2$. We used the following parameter values: $C = 1$, $g_L = -0.03$, $g_1 = 0.3$, $\tau = 40$, $V_{th} = 10$, $V_{rst} = -5$, $w_{rst} = -1$. Units are as in (Richardson et al. 2003; Rotstein 2013). **B.** The reset value w_{rst} changes according to the number of consecutive spikes (N) according to the following rule: when $N = N_{max}$, w_{rst} is decreased by an amount Δ_{wrst}. (The reset value V_{rst} is constant and independent of the number of spikes.) **B1.** $N_{max} = 2$ and $\Delta_{wrst} = 1.5$. **B2.** $N_{max} = 2$ and $\Delta_{wrst} = 2.5$. **B3.** $N_{max} = 2$ and $\Delta_{wrst} = 3$. **B4.** $N_{max} = 3$ and $\Delta_{wrst} = 2.1$. **B5.** $N_{max} = 3$ and $\Delta_{wrst} = 2.7$. **C.** The reset values V_{rst} and w_{rst} are constant and independent of the number of spikes (as in A). $I_{app} = -0.2 + \sqrt{2D}\eta(t)$ where last term is white noise (delta correlated) with zero mean and standard deviation D. We used $D = 0.2$. Other parameter values are as in A.

Figure 2. MMO patterns in 3D parabolic STO-F models with a parabolic nonlinearity in the voltage equation. The subthreshold dynamics is governed by the following three equations describing the dynamics of the rescaled voltage V (mv) and gating variables w and z: (i) $dV/dt = V^2 - w + I_{app}$, (ii) $\tau\, dw/dt = 0.5 * V - w$, and (iii) $\tau\, dz/dt = \eta$ (panels A) and $\tau\, dz/dt = \eta\,(0.5\, V +$

$0.02 - z$) (panels B). The onset of spikes is described by the equations describing the subthreshold dynamics. The occurrrence of spikes is indicated when V reaches V_{th} and V, w and z are reset to V_{rst}, w_{rst} and z_{rst} respectively. For $\eta = 0$, the corresponding 2D systems display damped STOs. **A1:** $I_{app} = -0.008$. **A2:** $I_{app} = -0.006$. **(A3):** $I_{app} = -0.004$. **B1:** $I_{app} = -0.004$. **B2:** $I_{app} = -0.003$. **(B3):** $I_{app} = -0.0027$. **B1:** $\gamma = 0.04$. **B2:** $\gamma = 0.06$. **B3:** $\gamma = 0.08$. We used the following parameters: $\tau = 100$, $\eta = 0.003$ (A), $\eta = 0.1$ (B), $V_{th} = 1$, $V_{rst} = -0.1$, $w_{rst} = V_{rst}^2 + I_{app} - 0.001$, and $z_{rst} = 0$.

Figure 3. STOs, spiking and MMOs in models of FitzHugh-Nagumo type. A. STOs ($\lambda = 0.0075$), and **B.** spiking ($\lambda = 0.008$) for the 2D FHN model described by the following equations: (i) $dv/dt = -2v^3 + 3v^2 - w$, (ii) $dw/dt = 0.01\,(4v - \lambda - w)$. **C.** MMOs for the extended, 3D FHN model described by the folllowing equations: (i) $dv/dt = -2v^3 + 3v^2 - w$, (ii) $dw/dt = 0.01\,(4v + 0.02 - z - w)$, (iii) $dz/dt = 0.0005\,(4v + 0.9 - z)$. Left panels: voltage time courses. Middle and right panels: Phase-planes. The right panels are magnifications of the middle ones. Panel C3 corresponds to the projection of the phase-space (for the variables v, w and z) onto the v-w plane.

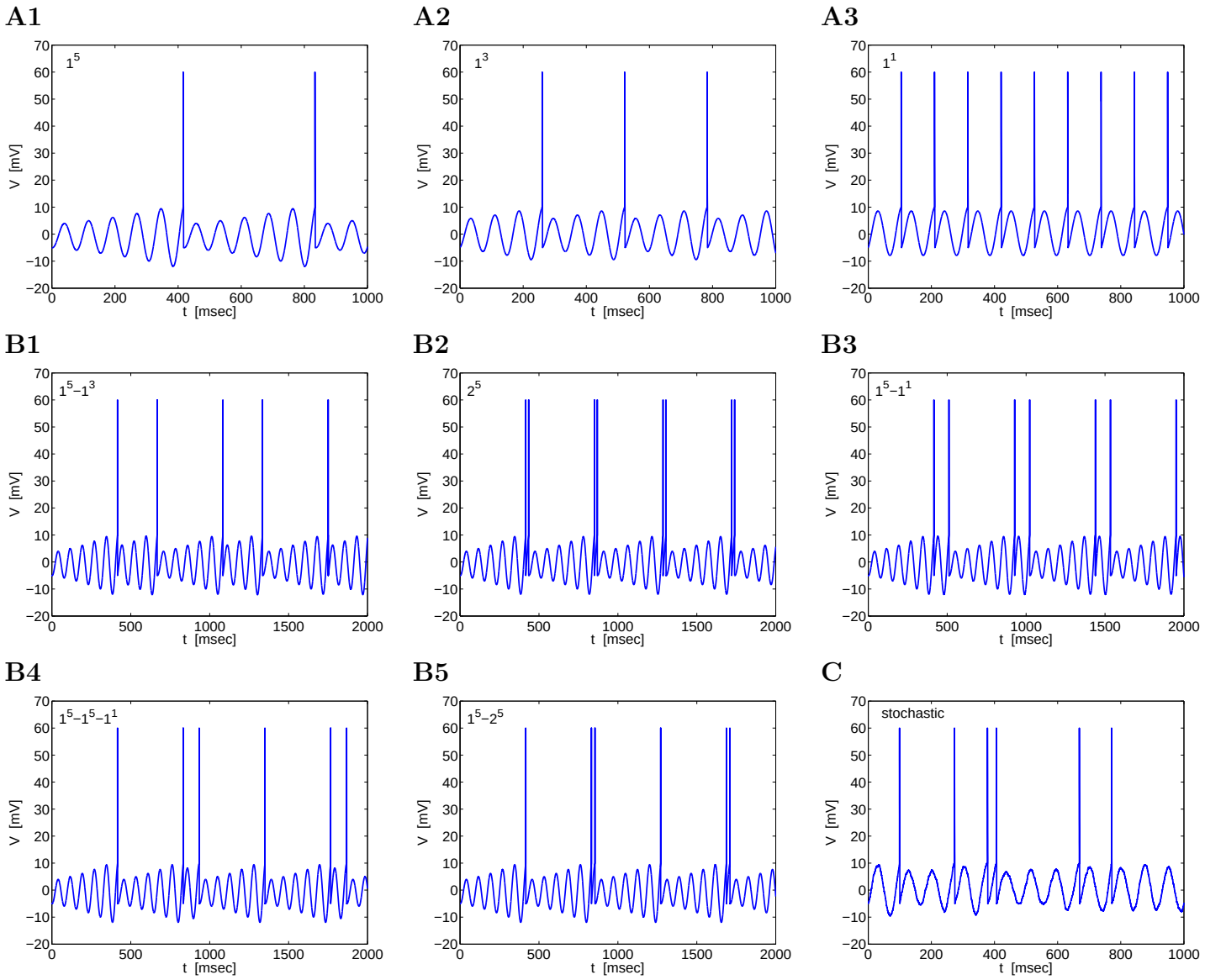

Figure 1: **MMO patterns in a 2D STO-F model with linear subthreshold dynamics**

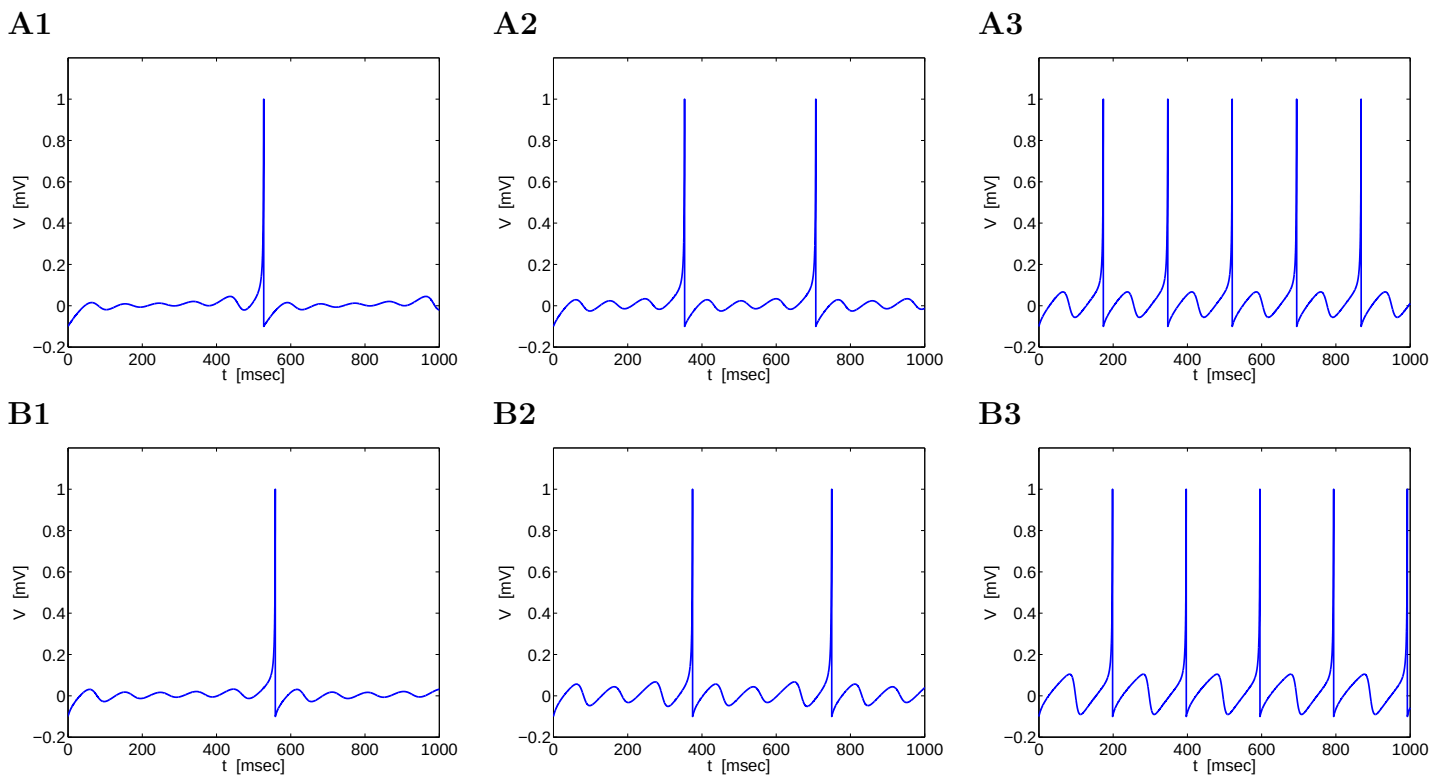

Figure 2: **MMO patterns in 3D STO-F models with a parabolic nonlinearity in the voltage equation.**

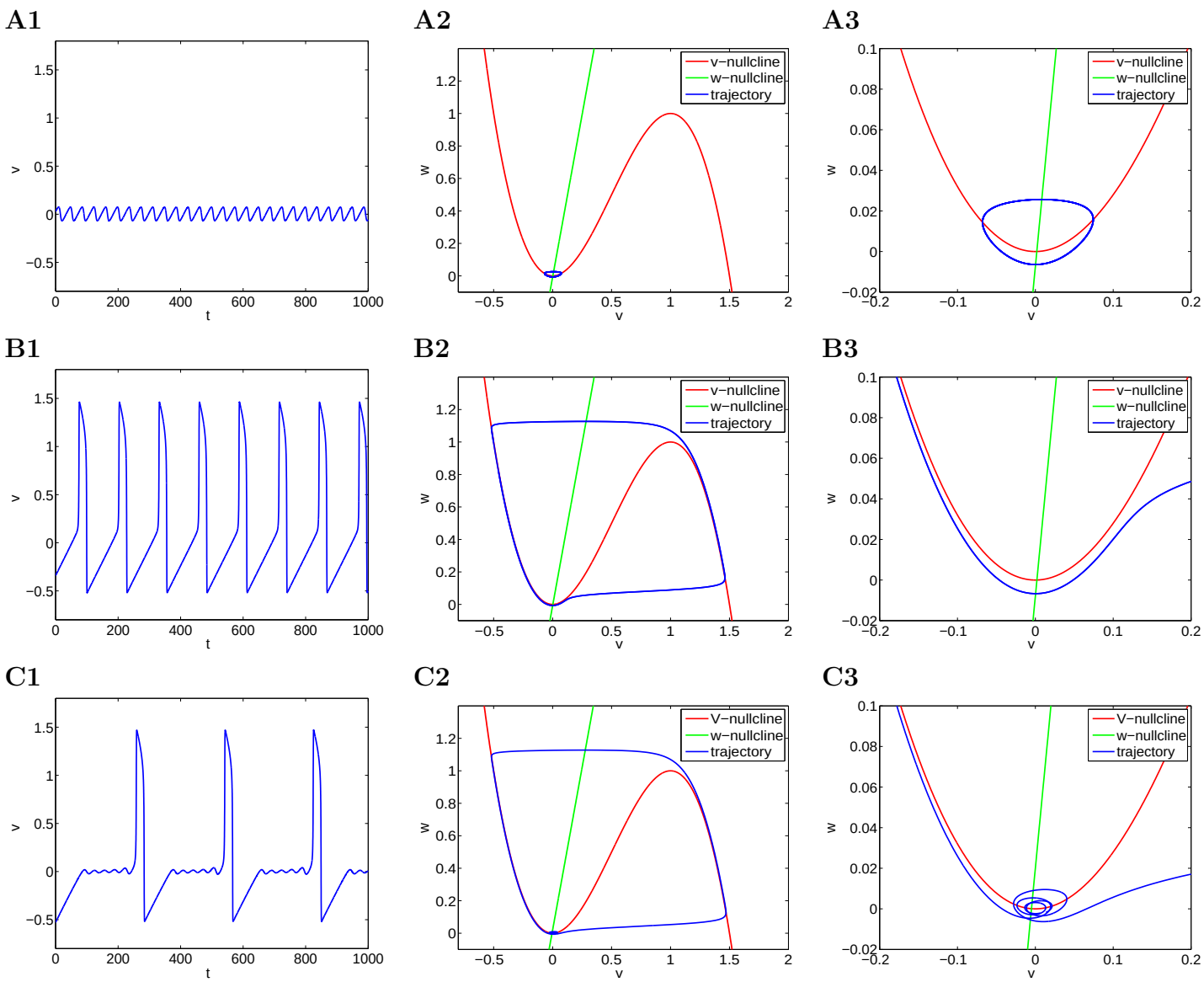

Figure 3: **STOs, spiking and MMOs in models of FitzHugh-Nagumo type.**